A Highly Regular Hexagonally Perforated Lamellar Structure in a Quiescent Diblock Copolymer

Yueh-Lin Loo[†] **and Richard A. Register***

Department of Chemical Engineering, Princeton University, Princeton, New Jersey 08544

Douglas H. Adamson

Princeton Institute for the Science and Technology of Materials, Princeton University, Princeton, New Jersey 08540

Anthony J. Ryan

The Polymer Centre, Department of Chemistry, University of Sheffield, Sheffield S3 7HF, United Kingdom

Received February 2, 2005
Revised Manuscript Received March 29, 2005

Introduction

The hexagonally perforated lamellar (HPL) structure in block copolymers has been the subject of considerable study and debate since its initial reports.[1−5] The interest in the HPL structure arises from its topology: as in the ordinary "unperforated" lamellar phase (L), each component is continuous in the plane of its lamellae, but hexagonally packed perforations through the lamellae formed by the minority component impart three-dimensional continuity to the majority component. No other diblock copolymer phase has this combination of 2D/3D continuity, which produces a distinct rheological response.[2] Moreover, selective removal of the minority component[6] from the HPL structure would generate an array of slitlike mesopores held open by pillars of the 3D-continuous majority component, whereas the L structure simply collapses when one component is removed.

Hajduk et al.[7] showed that the HPL structure is metastable with respect to the gyroid (G) phase in several bulk diblock copolymers, a conclusion supported by self-consistent-field calculations for the two structures, though the calculated free energy difference is quite small.[8,9] Previous observations of the HPL structure have often found poorly ordered structures, perhaps reflecting this metastability; indeed, Hajduk et al.[7] concluded that the order of the perforations was too poor in any of their unsheared samples to reliably distinguish the HPL structure from L. In the absence of regular order, the preferred pore spacing and stacking[10,11] (for example, ABAB vs ABCABC) cannot be determined. Alignment of the structure through large-amplitude shear often yields a regular pore arrangement,[5,12−15] but Zhu et al.[15] concluded that the stacking so developed was controlled by the shear, rather than being an intrinsic feature of the structure. Here, we describe a diblock copolymer system which spontaneously, rapidly, and reproducibly adopts a highly regular HPL structure, without any perturbing applied fields. We also find coexistence between L and HPL over a substantial temperature range (20 °C), with the relative fractions of the two structures depending uniquely on the temperature.

Experimental Section

The synthesis and molecular characterization of the two polystyrene−poly(ethylene-*alt*-propylene), S/EP, diblock copolymers studied here have been described previously.[16] In brief, the polymers were synthesized by sequential anionic polymerization of styrene and then isoprene, and the polyisoprene block selectively hydrogenated to EP. Both have polydispersities of 1.04 or less and no detectable homopolymer. S/EP 9/14 has a total weight-average molecular weight M_w = 22.5 kg/mol and an EP volume fraction $\phi_{EP} = 0.667$ at 140 °C; S/EP 7/13 has $M_w = 20.7$ kg/mol and $\phi_{EP} = 0.709$. Small-angle X-ray scattering (SAXS) data were acquired on beamline 8.2 of the Synchrotron Radiation Source (Daresbury Laboratory, Warrington, UK),[17] using an incident X-ray beam of wavelength $\lambda = 0.154$ nm. Data are presented against the magnitude of the momentum transfer vector $q \equiv (4\pi/\lambda) \sin \theta$, where θ is half the scattering angle. SAXS patterns were acquired with 6 s time resolution, using a Daresbury quadrant detector. The resolution (full width at half-maximum) of this system[18] is ≈ 0.017 nm^{-1}. A Linkam DSC600 stage controlled the sample temperature to within ±0.05 °C. The specimen for transmission electron microscopy (TEM) was prepared by heating a 1 mm thick film of a 2:1 w/w blend of S/EP 7/13 and S/EP 9/14 to 160 °C, holding for 1 h, and then quenching in liquid nitrogen. SAXS patterns taken at 160 °C, and subsequently at room temperature, confirmed that no morphological change occurred during the quench. A portion of this thick film was then immersed in aqueous RuO_4 (0.5 wt %) overnight to selectively stain the S domains. After embedding in acrylic resin, thin sections were prepared by microtoming at room temperature and examined on a Zeiss 910 TEM in bright field.[19]

Results and Discussion

Our previous examination of S/EP 9/14, via lower-resolution SAXS with a Kratky camera, revealed a low-temperature L phase.[16] Above 230 °C, the second-order SAXS peak diminished suddenly in intensity, suggesting the presence of another lamellar phase, which we termed L′, while further heating to 290 °C quickly transformed the L′ structure to G.[16] As discussed further below, the L′ structure in S/EP 9/14 transforms rapidly to L upon cooling, so that it was impossible to quench the structure to room temperature for TEM examination. However, our previous results[16] showed that the L ↔ L′ transition temperature decreased rapidly with an increase in ϕ_{EP}; a 2:1 w/w blend of S/EP 7/13 and S/EP 9/14 (with $\phi_{EP} = 0.696$) could be quenched from 160 °C to room temperature with the L′ structure intact. Two TEM images of this blend are shown in Figure 1; the extremely thin region shown on the left, containing only a single S layer, clearly confirms the existence and hexagonal arrangement of circular perforations through the S lamellae. This confirms our earlier suggestion[16] that the L′ phase has the HPL structure. The stacking (ABAB vs ABCABC) in the blend is unclear from the TEM image alone and is better investigated by SAXS.

The top trace in Figure 2 shows the high-resolution SAXS pattern for S/EP 9/14 at 260 °C. Seven peaks and shoulders are clearly evident, all of which can be indexed (within 0.001 nm^{-1} in q, for the five fully resolved peaks) according to the HPL structure with an

[†] Present address: Department of Chemical Engineering, The University of Texas at Austin, Austin, TX 78712.

* To whom correspondence should be addressed: e-mail register@princeton.edu.

10.1021/ma0502371 CCC: $30.25
Published on Web 05/06/2005

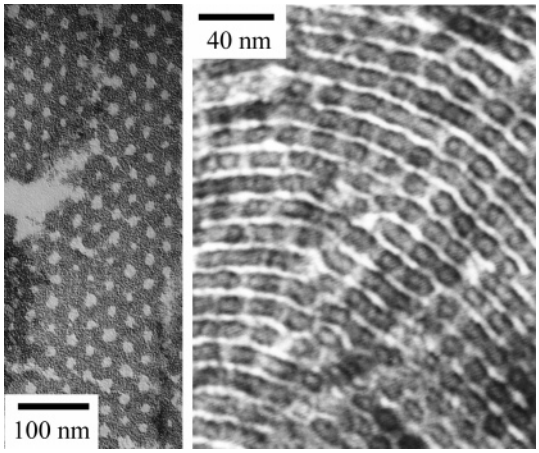

Figure 1. TEM images of thin sections of a 2:1 w/w blend of S/EP 7/13 and S/EP 9/14, exhibiting the HPL structure. S domains are stained dark with RuO_4. Left: an exceptionally thin region of the section, showing only a single S layer in plan view; the hexagonal arrangement of the light EP perforations is clearly evident. Right: an area of the section cut roughly normal to the layers; perforations are evident by the variation in darkness and thickness of the S layers.

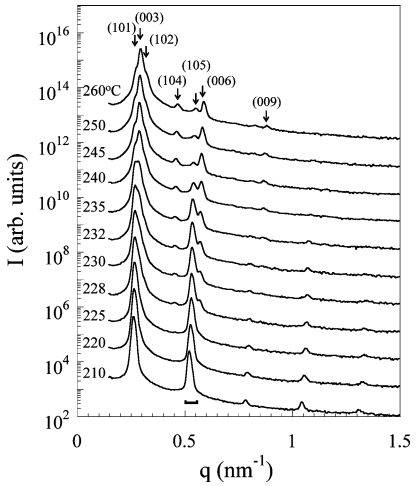

Figure 2. SAXS patterns for S/EP 9/14, at the temperatures indicated at left. Each pattern is the average of several 6 s frames, beginning once the SAXS pattern had stabilized. Indices ($h0l$) at top identify the peaks in the HPL structure, according to an ABCABC stacking of the perforations. Successive SAXS profiles are shifted by a decade in intensity for clarity.

ABCABC stacking. The hexagonal basis vector length (spacing between pores) is $a = 28.7$ nm, while the repeat distance along the lamellar normal is $c = 64.2$ nm (one ABC repeat, containing three S and three EP lamellae). Most of the reflections can also be indexed with an ABAB stacking (with $a = 27.0$ nm, $c = 42.8$ nm); the distinguishing feature is the shoulder observed near $q = 0.32$ nm^{-1} (marked as (102) in Figure 2), where no reflection exists for the ABAB stacking, indicating that little if any of the material stacks ABAB. Our measured c/a ratio (2.24) is quite similar to that found by Zhu et al.[15] (2.13) for the ABCABC-stacked fraction of a shear-oriented polystyrene/poly(ethylene oxide) diblock and by Ahn and Zin[14] (2.2) in a shear-oriented polystyrene/polyisoprene diblock, all of which are slightly below the value for a face-centered-cubic arrangement of the perforations ($c/a = \sqrt{6} = 2.45$).

The SAXS patterns in Figure 2 indicate that the HPL structure prevails from 245 to 260 °C, with only a small change in lattice spacing as the temperature is varied. Similarly, at 220 °C and below, the structure is L, as evidenced by the strong second-order reflection and the presence of reflections out to at least the fifth order. Conceptually, the L structure can be converted to HPL simply by opening pores,[20] without the need for chains to diffuse between layers; in this case, the (006) peak in the HPL structure would derive from the second-order peak in the L phase. Figure 3 shows how the positions of the second-order L and (006) HPL reflections change with temperature: the peak position, q_2, increases by 7% (layer spacing decreases by 7%) when L transforms to HPL. This is in excellent agreement with previous results showing a reduction in layer spacing during the L → HPL transition by 5−9% in other bulk diblocks.[13,21] Thus, the L → HPL transformation involves extensive overall rearrangement of the structure, with a significant change in the number of layers present, not merely a puncturing of the layers.

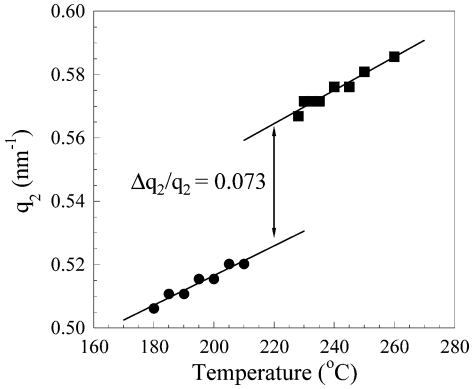

Figure 3. Position of the second-order peak, q_2, as a function of temperature: circles, second-order reflection from the L structure; squares, (006) reflection from the HPL structure. Note the 7% increase in q_2 when L transforms to HPL.

More interestingly, the SAXS patterns in Figure 2 change progressively between 220 and 245 °C, with the HPL reflections growing and the L reflections subsiding as the temperature is raised. One might infer that this simply reflects slow transformation kinetics, with a sharp L/HPL phase boundary located near 220 °C. However, this is not the case, as the data sets in Figure 2 were acquired in a random temperature sequence, by jumping between temperatures ranging from 180 to 260 °C. In S/EP 9/14, the transformation is remarkably rapid: while Mani et al.[22] reported thermoreversibility on the time scale of hours for the L ↔ HPL transition in an unsheared S/EP/S triblock, the SAXS pattern for S/EP 9/14 stabilized in <1 min from the time the temperature jump or drop was initiated.

The speed of the transition is most evident by examining the SAXS intensity integrated over $0.50 < q < 0.56$ nm^{-1}, which corresponds to the strong second-order reflection in the L structure at 220 °C and the relatively weak (105) HPL reflection at 260 °C. These chronological, frame-by-frame integrated intensity values are plotted at the top of Figure 4, with the temperature profile shown at the bottom. At 245 °C and above, the integrated intensity is essentially independent of temperature, reflecting the constancy of the SAXS profiles shown in Figure 2. A similar situation is found at 220 °C and below, where the L phase prevails and the integrated intensity depends only weakly on temperature. But between 220 and 245 °C, the integrated intensity changes dramatically; even a 3 °C temperature

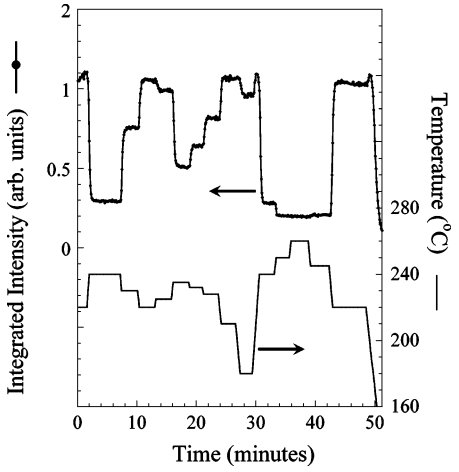

Figure 4. Stable coexistence of HPL and L structures. Bottom profile (right axis) shows the temperature profile employed, consisting of multiple temperature jumps and drops in random sequence, with isothermal holds in between. Top profile (left axis) shows the corresponding SAXS intensity integrated over $0.50 < q < 0.56$ nm^{-1}, the region indicated by the bar at the bottom of Figure 2. Each data point represents a single 6 s frame.

step produces an easily resolvable intensity change. Moreover, at each temperature in this range, the integrated intensity shows a particular value, which is reached rapidly and is independent of the thermal history: whether the sample was cooled or heated and whether the temperature jump/drop crossed the 220 °C threshold above which the signature of the HPL structure becomes visible.

One might also speculate that from 220 to 245 °C the lamellae develop modulations[5,12] of increasing amplitude, eventually yielding complete perforations at high temperature. In this case, the second-order peak in the L structure should transform smoothly into the HPL (006) reflection, increasing rapidly but smoothly in q over this temperature range to accommodate the 7% change in spacing evident in Figure 3. Instead, the SAXS patterns in Figure 2 are a simple superposition of HPL and L patterns, each with the relatively weak temperature dependence of the layer spacing indicated by the solid lines in Figure 3. This indicates coexistence of the L and HPL structures from 220 to 245 °C, with the balance shifting progressively toward HPL as the temperature is raised from 220 °C (no HPL) to 245 °C (all HPL).

Even anionically polymerized block copolymers show compositional polydispersity between chains,[21] which in principle permits equilibrium coexistence of ordered phases. However, such coexistence implies that the chains can "sort themselves" into domains different in local composition (ϕ_{EP}) which are still large enough to scatter coherently (e.g., micron-scale grains). Such a process seems highly unlikely, especially in times < 1 min. At present, we do not have a satisfying explanation for the behavior of the system in this temperature range, but we speculate that this feature may result from a persistent grain structure in these unoriented films, i.e., that transformations between L and HPL do not readily cross grain boundaries. For any phase transition, the transition temperature depends on the grain size through the Gibbs−Thomson equation.[23] It is possible that for the L ↔ HpL transition the interfacial energy and the transition enthalpy combine to produce an unusually strong size dependence of the transition temperature.

Though S/EP 9/14 can be reversibly and rapidly cycled between the L and HPL structures, this does not prove that HPL is an equilibrium phase. In other words, while the L ↔ HPL transition is rapid, this does not mean that the HPL ↔ G transition is rapid; transformations to and from the G phase are frequently sluggish.[24] Quenching S/EP 9/14 from the G phase at 290 to 230 °C did not produce any signature of the HPL structure even after 7 h,[25] so it is entirely plausible that the equilibrium structure above 220 °C is G, while HPL is an exceptionally long-lived (and in our case, well-ordered) metastable structure.[7]

Acknowledgment. The authors thank Dr. Chiajen Lai for the hydrogenation and molecular characterization of both diblock copolymers. This work was generously supported by the National Science Foundation through the Polymers Program (DMR-9711436 and DMR-0220236 to R.A.R.) and the Princeton Center for Complex Materials (DMR-9809483 and DMR-0213706). Daresbury beamtime was provided by the EPSRC under Grant GR/M22116 to A.J.R.

References and Notes

(1) Hashimoto, T.; Koizumi, S.; Hasegawa, H.; Izumitani, T.; Hyde, S. T. *Macromolecules* **1992**, *25*, 1433.
(2) Almdal, K.; Koppi, K. A.; Bates, F. S.; Mortensen, K. *Macromolecules* **1992**, *25*, 1743.
(3) Spontak, R. J.; Smith, S. D.; Ashraf, A. *Macromolecules* **1993**, *26*, 956.
(4) Disko, M. M.; Liang, K. S.; Behal, S. K.; Roe, R. J.; Jeon, K. J. *Macromolecules* **1993**, *26*, 2983.
(5) Hamley, I. W.; Koppi, K. A.; Rosedale, J. H.; Bates, F. S.; Almdal, K.; Mortensen, K. *Macromolecules* **1993**, *26*, 5959.
(6) Lee, J.-S.; Hirao, A.; Nakahama, S. *Macromolecules* **1989**, *22*, 2602.
(7) Hajduk, D. A.; Takenouchi, H.; Hillmyer, M. A.; Bates, F. S.; Vigild, M. E.; Almdal, K. A. *Macromolecules* **1997**, *30*, 3788.
(8) Matsen, M. W.; Schick, M. *Phys. Rev. Lett.* **1994**, *72*, 2660.
(9) Matsen, M. W.; Bates, F. S. *J. Chem. Phys.* **1997**, *106*, 2436.
(10) Förster, S.; Khandpur, A. K.; Zhao, J.; Bates, F. S.; Hamley, I. W.; Ryan, A. J.; Bras, W. *Macromolecules* **1994**, *27*, 6922.
(11) Qi, S.; Wang, Z.-G. *Macromolecules* **1997**, *30*, 4491.
(12) Hamley, I. W.; Gehlsen, M. D.; Khandpur, A. K.; Koppi, K. A.; Rosedale, J. H.; Schulz, M. F.; Bates, F. S.; Almdal, K.; Mortensen, K. *J. Phys. II* **1994**, *4*, 2161.
(13) Hajduk, D. A.; Ho, R.-M.; Hillmyer, M. A.; Bates, F. S.; Almdal, K. *J. Phys. Chem. B* **1998**, *102*, 1356.
(14) Ahn, J.-H.; Zin, W. C. *Macromolecules* **2000**, *33*, 641.
(15) Zhu, L.; Huang, P.; Cheng, S. Z. D.; Ge, Q.; Quirk, R. P.; Thomas, E. L.; Lotz, B.; Wittman, J.-C.; Hsiao, B. S.; Yeh, F.; Liu, L. *Phys. Rev. Lett.* **2001**, *86*, 6030.
(16) Lai, C.; Russel, W. B.; Register, R. A.; Marchand, G. R.; Adamson, D. H. *Macromolecules* **2000**, *33*, 3461.
(17) Bras, W.; Derbyshire, G. E.; Devine, A.; Clark, S. M.; Cooke, J.; Komanschek, B. E.; Ryan, A. J. *J. Appl. Crystallogr.* **1995**, *28*, 26.
(18) Mai, S.-M.; Fairclough, J. P. A.; Hamley, I. W.; Matsen, M. W.; Denny, R. C.; Liao, B.-X.; Booth, C.; Ryan, A. J. *Macromolecules* **1996**, *29*, 6212.
(19) Loo, Y.-L.; Register, R. A.; Adamson, D. H. *J. Polym. Sci., Part B: Polym. Phys.* **2000**, *38*, 2564.
(20) Qi, S.; Wang, Z.-G. *Phys. Rev. E* **1997**, *55*, 1682.
(21) Park, S.; Kwon, K.; Cho, D.; Lee, B.; Ree, M.; Chang, T. *Macromolecules* **2003**, *36*, 4662.
(22) Mani, S.; Weiss, R. A.; Cantino, M. E.; Khairallah, L. H.; Hahn, S. F.; Williams, C. E. *Eur. Polym. J.* **2000**, *36*, 215.
(23) Floudas, G.; Pakula, T.; Velis, G.; Sioula, S.; Hadjichristidis, N. *J. Chem. Phys.* **1998**, *108*, 6498.
(24) Vigild, M. E.; Almdal, K.; Mortensen, K.; Hamley, I. W.; Fairclough, J. P. A.; Ryan, A. J. *Macromolecules* **1998**, *31*, 5702.
(25) Lai, C.; Register, R. A., unpublished data.

MA050237L